DESY 99–125
MZ-TH/99–36
TTP99-35
hep–ph/9909230
August 1999

ISSN 0418–9833

Deep Inelastic $e\gamma$ Scattering at High Q^2

A. Gehrmann-De Ridder[1,2], H. Spiesberger[3] and
P. M. Zerwas[1]

[1] Deutsches Elektronen-Synchrotron DESY, D-22603 Hamburg, Germany

[2] Institut für Theoretische Teilchenphysik, Universität Karlsruhe,
D-76128 Karlsruhe, Germany

[3] Institut für Physik, Johannes-Gutenberg-Universität,
Staudinger Weg 7, D-55099 Mainz, Germany

Abstract

The electromagnetic and weak structure functions of the photon can be studied in the deep inelastic electron-photon processes $e\gamma \to e + X$ and $e\gamma \to \nu + X$. While at low energies only virtual photon exchange is operative in the neutral-current process, additional Z-exchange becomes relevant for high Q^2 of order M_Z^2 at e^+e^- linear colliders. Likewise the charged-current process can be observed at these high energy colliders. By measuring the electroweak neutral- and charged-current structure functions, the up- and down-type quark content of the photon can be determined separately.

1. The photon structure functions, which can be measured in deep-inelastic electron-photon scattering [1], are an area of theoretically exciting QCD phenomena. In contrast to the structure function of the proton, the transverse structure function of the photon is predicted to rise linearly with the logarithm of the momentum transfer Q^2 and to increase with increasing Bjorken x [2]. The quark-parton prediction is renormalized in QCD by gluon bremsstrahlung to order unity without altering the basic characteristics, and the absolute magnitude of the photon structure function is asymptotically determined by the QCD coupling [3]. The characteristic features of the photon structure function F_2^γ are borne out by experimental data [4] though significant improvement of the experimental accuracy is still demanded.

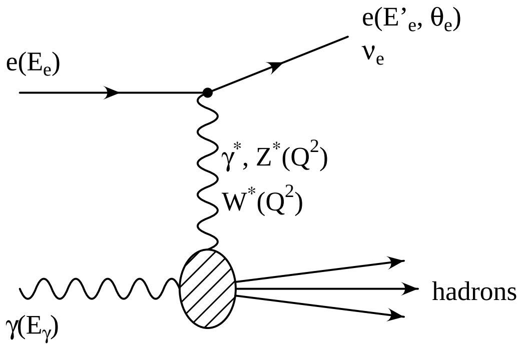

Figure 1: *Kinematics of deep-inelastic electron-γ scattering.*

At large momentum transfer Q^2 of the order of the Z, W masses squared, the neutral-current (NC) $e\gamma$ process becomes sensitive to the exchange of virtual Z^* bosons in addition to the virtual γ^* photon; moreover the charged-current (CC) process, mediated by virtual W^* exchange, becomes experimentally accessible [5, 6]:

$$e+\gamma \quad \xrightarrow{\gamma^*,Z^*} \quad e+X \tag{1}$$

$$e+\gamma \quad \xrightarrow{W^*} \quad \nu+X \tag{2}$$

These processes can be studied at e^+e^- linear colliders [7] where the high energy γ beams can be generated by Compton back-scattering of laser light [8]. When exploring the quark structure of the photon by virtual photons, up- and down-type quarks are probed at a fixed ratio 4:1. However, since the weak charges of the quarks differ from the electric charges, the mechanisms (1) and (2) can be exploited to determine the up- and down-type quark content of the photon separately at high Q^2. These measurements are an interesting task since for asymptotic energies the up/down quark decomposition of the photon can be predicted by QCD.

2. The differential cross section of the NC process for unpolarized leptons and photons is parametrized by two structure functions $F_2^{\gamma,\mathrm{NC}}$ and $F_L^{\gamma,\mathrm{NC}}$:

$$\frac{d^2\sigma}{dxdQ^2}\left[e^\pm+\gamma\to e^\pm+X\right]=\frac{2\pi\alpha^2}{Q^4}\frac{1}{x}\left\{\left[1+(1-y)^2\right]F_2^{\gamma,\mathrm{NC}}-y^2F_L^{\gamma,\mathrm{NC}}\right\} \tag{3}$$

while the CC process is parametrized by three structure functions $F_2^{\gamma,\mathrm{CC}}$, $F_L^{\gamma,\mathrm{CC}}$ and $F_3^{\gamma,\mathrm{CC}}$:

$$\frac{d^2\sigma}{dxdQ^2}\Big[e^\pm+\gamma\to\overset{(-)}{\nu}+X\Big]=$$
$$\frac{G_F^2}{4\pi}\left[\frac{M_W^2}{Q^2+M_W^2}\right]^2\frac{1}{x}\left\{\left[1+(1-y)^2\right]F_2^{\gamma,\mathrm{CC}}\mp\left[1-(1-y)^2\right]xF_3^{\gamma,\mathrm{CC}}-y^2F_L^{\gamma,\mathrm{CC}}\right\} \quad (4)$$

α is the electromagnetic coupling defined at the scale Q^2, G_F the Fermi coupling; M_W and $\sin^2\theta_w$ are the W mass and the electroweak mixing angle. The momentum transfer Q^2, the Bjorken variable $x=Q^2/2q\cdot p_\gamma$ and $y=q\cdot p_\gamma/k\cdot p_\gamma$ (with p_γ, q denoting the γ, γ^* and k the incoming lepton four-momenta) can be expressed in terms of the electron energies E_e, E_e', the scattering angle of the electron Θ_e and the invariant hadron energy W_h in the final state for the NC process:

$$\begin{aligned}\mathbf{NC}: \qquad Q^2 &= 2E_eE_e'(1-\cos\Theta_e)\\ x &= Q^2/(Q^2+W_h^2)\\ y &= 1-E_e'/E_e\cos^2\Theta_e/2\end{aligned}$$

For the CC process, including the invisible neutrino in the final state, the Blondel-Jacquet representation of these variables must be used, defined in terms of hadron momenta in the final state [9]:

$$\begin{aligned}\mathbf{CC}: \qquad Q^2 &= p_{\perp h}^2/(1-y)\\ x &= Q^2/(Q^2+W_h^2)\\ y &= (E_h-p_h)/E_h\end{aligned}$$

E_h, p_h and $p_{\perp h}$ are the sum of hadron energies and of longitudinal and transverse momenta in the laboratory frame with respect to the beam axis. The analysis of the structure functions does not depend on the γ spectrum of the initial state in either case; in fact, the invariant $(e\gamma)$ energy can be reconstructed on an event-by-event basis from the momentum transfer and the scaling variables, $s_{e\gamma}=Q^2/(xy)$. Experimental observation of the events requires minimal scattering angles in the NC process and hadron angles in the final state of the CC process. In practice this restricts Q^2 to more than 50 GeV^2.

3. Restricting ourselves in this letter[1] to leading-order QCD predictions which have been proven in Ref. [10] to be quite accurate, the relevant structure functions $F_2^{\gamma,\mathrm{NC}}$, $F_2^{\gamma,\mathrm{CC}}$, and $xF_3^{\gamma,\mathrm{CC}}$ for electron scattering can be expressed by the densities of the light quark species $u,..\ b$:

$$F_2^{\gamma,\mathrm{NC}}=2\sum_q\hat{e}_q^2x\ q(x,Q^2) \quad (5)$$

[1]In an extended version of this paper we will present a complete analysis of QCD corrections in next-to-leading order as well as an elaborate account of CKM and mass effects for heavy quark final states.

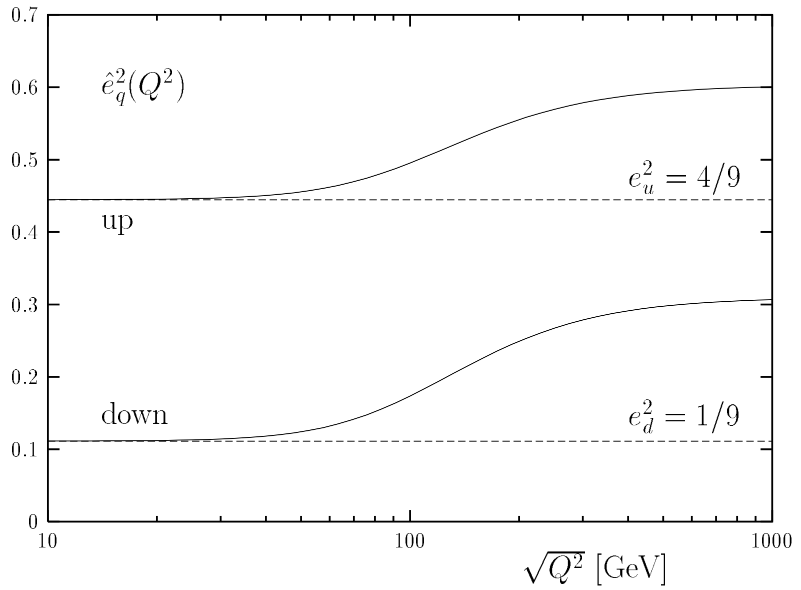

Figure 2: *The up and down effective charges as a function of* $\sqrt{Q^2}$.

and

$$\begin{aligned} F_2^{\gamma,\mathrm{CC}} &= x\,(u+c+d+s) \\ xF_3^{\gamma,\mathrm{CC}} &= x\,(u+c-d-s) \end{aligned} \tag{6}$$

In this representation, use has been made of $\bar{q} = q$ for the quark distributions in the photon. The charged-current structure functions for positron scattering are obtained from (6) by exchanging up- and down-type quarks. The effective charges $\hat{e}_q$ are given by the coherent superposition of the electric γ and the electroweak left- and right-chiral Z charges:

$$\hat{e}_q^2 = \frac{1}{4}\sum_{i,j=L,R}\left[e_q - \frac{Q^2}{Q^2+M_Z^2}\frac{z_i(e)z_j(q)}{\sin^2\theta_w\cos^2\theta_w}\right]^2 \tag{7}$$

with

$$\begin{aligned} z_L(f) &= I_{3L}(f) - e_f\sin^2\theta_w \\ z_R(f) &= \phantom{I_{3L}(f)} - e_f\sin^2\theta_w \end{aligned}$$

The modification of the electric charge e_q^2 to the effective charge $\hat{e}_q^2$ becomes increasingly important at Q^2 above 10^3 GeV^2. Anticipating that experiments may be feasible up to Q^2 of order of 10^5 GeV^2 at 500 GeV colliders (see [7] for experimental simulations), and of order 10^6 GeV^2 at 1 TeV colliders, the Q^2 evolution of the effective charges $\hat{e}_u^2$ and $\hat{e}_d^2$ in the transition zone is illustrated in Fig. 2. $\hat{e}_u^2$ evolves from 4/9 asymptotically to 0.60 and $\hat{e}_d^2$ from 1/9 to 0.31.

Based on the lowest-order QCD representation, the NC and CC cross sections for

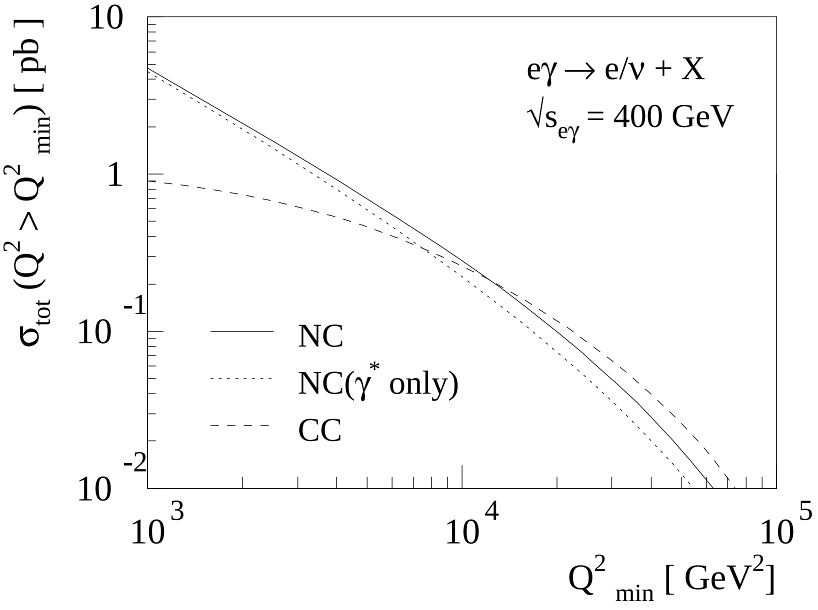

Figure 3: *The deep inelastic* $e\gamma$ *cross sections as a function of* $Q^2_{\rm min}$ *for the* $e\gamma$ *collider energy* $\sqrt{s_{e\gamma}} = 400$ *GeV; parton densities: Ref. [12].*

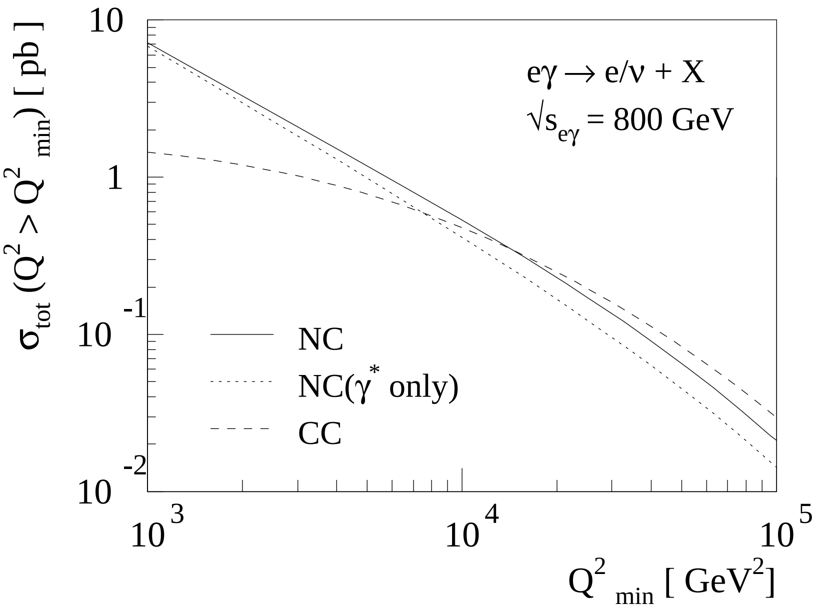

Figure 4: *The deep inelastic* $e\gamma$ *cross sections as a function of* $Q^2_{\rm min}$ *for the* $e\gamma$ *collider energy* $\sqrt{s_{e\gamma}} = 800$ *GeV; parton densities: Ref. [12].*

electron and positron scattering can be written in a simple form in the variables x, y [5]:

$$\frac{\mathrm{d}\sigma}{\mathrm{d}x\mathrm{d}y}[e\gamma \to eX] = \frac{2\pi\alpha^2 s_{e\gamma}}{Q^4}\left[1+(1-y)^2\right]\sum_q \hat{e}_q^2\, x\, q(x,Q^2) \tag{8}$$

$$\frac{\mathrm{d}\sigma}{\mathrm{d}x\mathrm{d}y}[e\gamma \to \nu X] = \frac{G_F^2 s_{e\gamma}}{2\pi}\left[\frac{M_W^2}{M_W^2+Q^2}\right]^2 x\left[(u+c)+(1-y)^2(d+s)\right] \tag{9}$$

The cross sections for electron and positron beams are equal by $\mathcal{CP}$ invariance.

The size of the cross sections is shown in Fig. 3 and Fig. 4 for the NC and CC processes. The differential cross sections (8, 9) are integrated down to a minimum $Q^2_{min} \leq xys_{e\gamma}$ for fixed[2] initial γ energies $E_\gamma = 0.8E_e$ and electron beam energies $E_e = 250$ GeV and 0.5 TeV [7]. The full curves correspond to the NC cross section obtained with the parametrization of Ref. [12] in which the parton densities are evolved from an ansatz defined at low Q^2; the dotted lines indicate the electromagnetic component of the NC cross section. Due to the Z exchange, the cross section increases by 25 % for $Q^2_{\mathrm{min}} = 5\times 10^4$ GeV^2 at $\sqrt{s_{e\gamma}} = 400$ GeV. The dashed lines correspond to the CC cross section. Similar predictions follow from the parametrization [13].

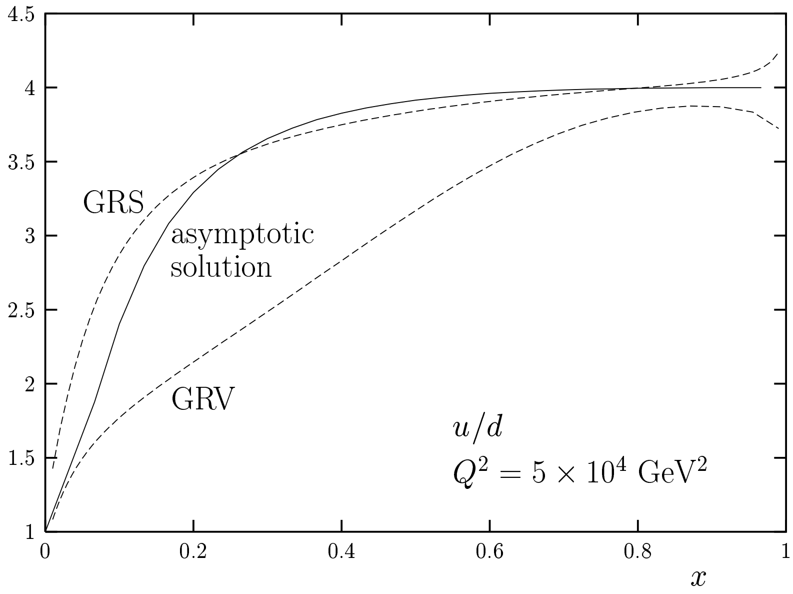

Figure 5: *The ratio of the u to d quarks content in the photon as a function of x at $Q^2 = 5\times 10^4$ GeV^2 using the leading-order parametrizations of Ref. [12] (GRV) and Ref. [13] (GRS). The asymptotic solution [3] is indicated by the full line.*

[2]Choosing the laser and electron/positron beams to have opposite helicities $\lambda_e\lambda_\gamma = -1/2$ [8, 11], and separating spatially the conversion from the reaction point, the γ spectrum in Compton backscattering of laser light can be tuned sharply with small band width near $E_\gamma/E_e \simeq 0.8$ for proper laser colors. The high-energy γ beam is unpolarized when the initial laser and lepton helicities are flipped at the same time.

4. Examining the predicted size of the cross sections in Fig. 3 and Fig. 4, it is obvious that the NC and CC processes can be investigated for an experimentally large range of Q^2. With the expected $e\gamma$ luminosity in excess of $\int L \gtrsim 100 fb^{-1}/a$ in a high-luminosity machine, such as TESLA [14], a cross section of size $\sigma \sim 10^{-1}$ pb gives rise to a sample of $\sim 10^4$ events per year. The effect of the Z exchange on the NC process and the CC process can be exploited to separate the up- and down-type quark components of the photon, as evident from the cross sections (8, 9). The separation will allow to examine the initial conditions for the evolution of the parton densities from low Q^2 values. Choosing an incoherent instead of a coherent superposition of vector-meson states leads to quite different u/d ratios. While in the valence region the ratio of u to d quarks in the photon is expected to be 4:1, the ratio should approach 1:1 when the evolution to democratically distributed sea quarks is fully operative. Involving a two-step splitting process $q \to g \to q'$, the transition can only be observed for sufficiently small x as exemplified in Fig. 5 for the parametrizations of Refs. [12, 13] at $Q^2 = 5 \times 10^4$ GeV^2 and the asymptotic solution. x values down to order 10^{-2} will be accessible at these colliders even for large Q^2 values.

Acknowledgements

We thank D. J. Miller for very useful discussions on experimental aspects of this analysis, and we thank G. Blair for valuable comments on the manuscript. A. G. is grateful to A. Wagner for financial support during her stay at DESY where part of this work was carried out.

References

[1] T. F. Walsh, Phys. Lett. **B36** (1971) 121; S. J. Brodsky, T. Kinoshita and H. Terazawa, Phys. Rev. Lett. **27** (1971) 280.

[2] T. F. Walsh and P. M. Zerwas, Phys. Lett. **B44** (1973) 196.

[3] E. Witten, Nucl. Phys. **B120** (1977) 189.

[4] Ch. Berger and W. Wagner, Phys. Rep. **C146** (1987) 1; H. Kolanoski and P. M. Zerwas, in "High Energy Electron-Positron Physics", eds. A. Ali and P. Söding, World Scientific (1988); R. Nisius, Proceedings, *Int. Conference on the Structure and Interactions of the Photon*, Freiburg 1999, to appear in Nucl. Phys. Proc. Suppl. **B**.

[5] A. Cordier and P. M. Zerwas, Proceedings, *EFCA Workshop on LEP200*, Aachen 1986, eds. A. Böhm and W. Hoogland, CERN Report 87-08; S. J. Brodsky, M. Krämer and P. M. Zerwas, Nucl. Phys. Proc. Suppl. **37B** (1994) 293.

[6] A. Gehrmann-De Ridder, Proceedings, *Int. Conference on the Structure and Interactions of the Photon*, Freiburg 1999, to appear in Nucl. Phys. Proc. Suppl. **B**, [hep-ph/9906547].

[7] E. Accomando et al., Phys. Rep. **299** (1998) 1; D. J. Miller and A. Vogt, Proceedings, *e^+e^- collisions at TeV Energies: The Physics Potential*, ed. P. M. Zerwas, DESY-96-123D; A. Vogt, Proceedings, *Int. Conference on the Structure and Interactions of the Photon*, Freiburg 1999, to appear in Nucl. Phys. Proc. Suppl. **B**.

[8] I. F. Ginzburg, G. L. Kotkin, S. L. Panfil, V. G. Serbo and V. I. Telnov, Nucl. Instr. and Meth. **219** (1984) 5.

[9] A. Blondel and F. Jacquet, Proceedings, *Study of an e-p Facility for Europe*, ed. U. Amaldi, DESY 79-48.

[10] M. Glück, E. Reya and A. Vogt, Phys. Rev. **D45** (1992) 3986.

[11] J. Kühn, E. Mirkes and J. Steegborn, Z. Phys. **C57** (1993) 615.

[12] M. Glück, E. Reya and A. Vogt, Phys. Rev. **D46** (1992) 1973.

[13] M. Glück, E. Reya and I. Schienbein, Phys. Rev. **D60** (1999) 054019.

[14] S. Söldner-Rembold, Proceedings, *Physics and Experiments with High Luminosity e^+e^- Linear Colliders*, eds. R. Heuer, F. Richard and P. M. Zerwas, DESY 99-123F (to appear); A. de Roeck, Proccedings, *1999 Workshop on Linear Colliders*, Sitges 1999, (to appear).